Solar Energy Materials & Solar Cells 96 (2012) 141–147

Contents lists available at SciVerse ScienceDirect

Solar Energy Materials & Solar Cells

journal homepage: www.elsevier.com/locate/solmat

ITO-free inverted polymer/fullerene solar cells: Interface effects and comparison of different semi-transparent front contacts

Sebastian Wilken *, Thomas Hoffmann, Elizabeth von Hauff [1], Holger Borchert, Jürgen Parisi

Carl von Ossietzky University of Oldenburg, Department of Physics, Energy and Semiconductor Research Laboratory, Carl-von-Ossietzky-Str. 9–11, 26129 Oldenburg, Germany

ARTICLE INFO

Article history:
Received 21 July 2011
Received in revised form
15 September 2011
Accepted 17 September 2011
Available online 10 October 2011

Keywords:
Polymer/fullerene solar cells
Inverted
Contacts
Interfaces
Simulation
Reproducibility

ABSTRACT

Polymer/fullerene solar cells with an inverted layer sequence and free from indium tin oxide (ITO) are presented in this study. We concentrate on critical interface effects in inverted devices and compare different semi-transparent front contacts, such as ultra-thin Au films and Au grid structures. The solvent of the absorber blend was found to have a distinct impact on the stability of the initially deposited cathode layer. Furthermore, we did wettability studies of poly(3,4-ethylenedioxythiophene):poly(4-styrenesulfonate) (PEDOT:PSS) on the active layer and determined the surface energy of polymer/fullerene blends. Ultra-thin Au films with varying thickness were investigated in terms of sheet resistance and transmittance. The optimal thickness was achieved via simulation of organic solar cells. Finally, we present a comparison of inverted solar cells with an active area of about 1 cm^2 both with Au films and Au grid structures as front contact in terms of photovoltaic performance, reproducibility, and degradation. Notably better results were achieved when using Au grid structures as front contact, even with a not optimized grid geometry.

1. Introduction

Organic solar cells (OSCs) provide considerable advantages over their inorganic counterparts such as possible cost-effective and environmentally compatible manufacturing, light weight applications, and flexibility. Tremendous scientific efforts were made in this field over the last few years, leading to certified power conversion efficiencies up to 8.3% nowadays [1]. The most commonly used material system for OSCs consists of conjugated polymers as the electron donor and fullerene derivates as the electron acceptor materials, blended in a bulk heterojunction (BHJ) to overcome the strong excitonic behavior of photogenerated charge carriers [2,3]. BHJ solar cells are solution-producible at low temperatures, which makes them feasible for roll-to-roll processing [4]. A medium scale manufacture and product integration of roll-to-roll processed OSCs has been demonstrated recently [5].

Polymer/fullerene solar cells are typically deposited on indium tin oxide (ITO) covered substrates, since ITO offers an excellent combination between electrical conductivity and transparency. An additional hole transport layer (HTL) is frequently used, in order to smooth the relatively rough ITO surface and match the highest occupied molecular orbital (HOMO) of the donor material to the work function of the ITO. Finally, a low work-function metal like Al is evaporated as cathode on top of the absorber blend. Several studies report about an inversion of this standard architecture in terms of converting ITO into the electron contact. This is usually realized by the incorporation of electron-selective materials like TiO_x or ZnO [6,7]. The hole contact is formed by high work-function metals like Ag and Au, in this case. Those devices promise a better long-term stability, in contrast to the standard setup with the reactive Al cathode exposed to air [8]. Besides this "classical" approach of inverted OSCs, much work has been done recently to establish ITO-free devices. ITO will feasibly become a bottleneck in large-scale production of OSCs, concerning the rapidly increasing demand for flat panel displays. Different concepts for alternative (semi-)transparent contacts are discussed in the literature, e.g. ultra-thin metal films [9–11], high-conductive polymers in combination with metal grids [12–14], metallic nanowires [15,16], and carbon nanotubes [17]. In recent studies a solution-based roll-to-roll processing of large-area ITO-free OSCs was established using Ag nanoparticles [18,19] as well as Kapton foils with an Al/Cr bilayer system [20] combined with screen printed Ag grids.

In this study, we focus on ITO-free inverted OSCs in substrate configuration (see Fig. 1) as described by Glatthaar et al. [12]. A blend of poly(3-hexylthiophene) (P3HT) and [6,6]-phenyl-C_{61}-butyric acid methyl ester (PCBM) was used as absorber layer. We

* Corresponding author. Tel.: +49 441 798 3749; fax: +49 441 798 3990.
E-mail address: sebastian.wilken@uni-oldenburg.de (S. Wilken).
[1] Present address: Institute of Physics, Albert-Ludwigs University of Freiburg, Hermann-Herder-Str. 3, 79104 Freiburg, Germany/Fraunhofer Institute for Solar Energy Systems (ISE), Heidenhofstr. 2, 79110 Freiburg, Germany.

0927-0248/$ - see front matter © 2011 Elsevier B.V. All rights reserved.
doi:10.1016/j.solmat.2011.09.044

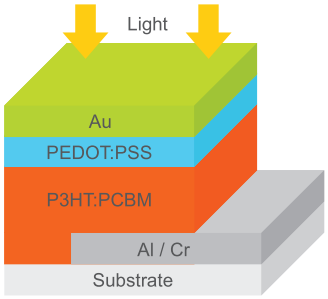

Fig. 1. Schematic setup of an inverted BHJ solar cell in substrate configuration with an absorber blend of P3HT:PCBM.

choose Al/Cr as the opaque cathode material, since a thin layer of Cr on top of the Al layer was found to be necessary, which we attribute to an impact of the P3HT:PCBM solvent on cathode stability. A high-conductive formulation of poly(3,4-ethylenedioxythiophene):poly(4-styrenesulfonate) (PEDOT:PSS) was used as HTL, in order to enhance lateral transport of charge carriers as well. With contact angle measurements, we observed that improved wetting of PEDOT:PSS on the absorber blend is crucial for inverted OSC performance. Therefore, we estimated the surface energy of pristine P3HT:PCBM films and studied the enhancement of wettability by merging PEDOT:PSS dispersions with alcohol solvents. Since the conductivity of PEDOT:PSS is still limited, we used two different concepts for charge carrier collection: ultra-thin Au films and Au grid structures, respectively. We present an approach to find the optimal thickness of Au films in terms of transmittance and sheet resistance and, finally, compare inverted OSCs with both contact configurations regarding photovoltaic performance, reproducibility, and degradation.

2. Experimental details

Inverted BHJ solar cells were fabricated on glass substrates. All preparation steps except the deposition of PEDOT:PSS were performed in a N_2 filled glovebox. Substrates were cleaned consecutively with detergent, acetone, and 2-propanol using an ultrasonic bath, followed by an O_2 plasma treatment for 10 min. The bottom contact was evaporated in sequence Cr (6 nm)/Al (100 nm)/Cr (12 nm). Thin layers of Cr were used to serve as adhesive agent and passivation layer, respectively. Subsequently, the absorber blend of P3HT (Merck) and PCBM (Solenne BV) in mixing ratio 1:1 by weight was spin-coated at 600 rpm from a 1 wt% solution in *ortho*-dichlorobenzene (oDCB). The solution was stirred at 80 °C for at least one day before usage. The resulting absorber thickness was about 100 nm. Afterwards, the samples were annealed at 150 °C for 10 min. The high-conductive PEDOT:PSS formulation Clevios CPP 105 D, purchased from H.C. Starck, was spin-coated on top of the absorber blend (two steps at 1500 rpm and 2000 rpm). This procedure was performed in ambient air, in order to protect the glovebox atmosphere against contamination with water. The resulting thickness of PEDOT:PSS was around 200 nm. Subsequently, the cells were tempered at (80 . . . 100) °C for 5 min. Finally, Au was evaporated as front contact through a shadow mask, either as semi-transparent thin film or 80 nm thick grid structure with a grating period of 2.25 mm and a width of 250 μm for each grid line.

Current density versus voltage (J–V) characteristics of inverted solar cells were recorded in ambient air and without encapsulation using an Advantest TR 6143 source measurement unit. The cells were illuminated with a solar simulator (K.H. Steuernagel Technical Lightning), providing a simulated AM1.5 spectrum. The light intensity was adjusted to 100 mW/cm^2 using a Si reference solar cell, calibrated at Fraunhofer ISE. The photoactive area was defined to $A \approx (1 \times 1)$ cm^2 by application of illumination masks. For basic stability investigations we employed the ISOS-L-1 standard laboratory test conditions [21]. Devices were kept under continuous illumination of 100 mW/cm^2 in ambient air with ambient temperature and humidity, while J–V characteristics were recorded in a fixed time interval.

Atomic force microscopy (AFM) measurements were performed on a Digital Instruments/Veeco Dimension 3100 microscope with Nanoscope IIIA Controller in tapping mode. Contact angles were measured using the sessile drop technique in a homemade setup based on a Nikon D40× digital camera. Drop profiles were analyzed with the public domain software ImageJ and the plug-in DropSnake [22]. Ultra-thin Au films were evaporated on glass substrates with a thickness ranging from 7 nm to 60 nm. UV/Vis transmittance spectra were recorded with a Varian Cary 100 spectrophotometer. Sheet resistance measurements were performed using the van der Pauw method [23]. The film thickness was controlled in situ during evaporation with a quartz crystal microbalance and validated afterwards using both a Veeco Dektak 6 M stylus profiler and an optical approach, as will be discussed later.

3. Theoretical aspects and simulation

3.1. Surface energy of solids

According to Fowkes [24], the surface tension σ_l of liquids as well as the surface energy σ_s of solids can be split up in dispersive (d) and polar (p) fractions

$$\sigma_l = \sigma_l^d + \sigma_l^p, \quad \sigma_s = \sigma_s^d + \sigma_s^p. \tag{1}$$

Owens, Wendt, Rabel, and Kaeble (OWRK) [25,26] introduced a technique to obtain σ_s by measuring the contact angle θ for several liquids with known values for σ_l^d and σ_l^p and plotting the data points in the form

$$\frac{(1+\cos\theta)\sigma_l}{2\sqrt{\sigma_l^d}} = \sqrt{\sigma_s^p}\sqrt{\frac{\sigma_l^p}{\sigma_l^d}} + \sqrt{\sigma_s^d}. \tag{2}$$

The dispersive and polar fractions of the solid's surface energy can be easily achieved via linear regression, according to Eq. (2).

3.2. Resistivity of ultra-thin metal films

The resistivity of ultra-thin metal films exceeds the specific resistivity ρ_0 of the bulk material due to scattering of electrons at surfaces and grain boundaries. Both effects strongly depend on film thickness t and can be quantified using the Fuchs–Sondheimer (FS) [27,28] and Mayadas–Shatzkes (MS) [29] models

$$\frac{\rho_{FS}}{\rho_0} = \left[1 - \frac{3}{2k}(1-p)\int_1^\infty \left(\frac{1}{t^3} - \frac{1}{t^5}\right)\frac{1-e^{-kt}}{1-pe^{-kt}}dt\right]^{-1}, \tag{3}$$

$$\frac{\rho_{MS}}{\rho_0} = \left[1 - \frac{3}{2}\alpha + 3\alpha^2 - 3\alpha^3 \ln\left(1+\frac{1}{\alpha}\right)\right]^{-1}. \tag{4}$$

Surface scattering (FS model) depends on $k = t/\lambda_0$, which is the ratio between thickness and mean free path length λ_0 of electrons, and $p = 0 \ldots 1$, describing whether the scattering is specular or diffusive. Grain boundary scattering (MS model) is depicted by $\alpha = (\lambda_0/D)\cdot R/(1-R)$ with the grain size D as function of t and the grain boundary reflection coefficient $R = 0 \ldots 1$. By analogy with Matthiessen's rule, both models can be combined expressing the